Electrocatalytic Pathways on Carbon-Supported Platinum Nanoparticles: Comparison of Particle-Size-Dependent Rates of Methanol, Formic Acid, and Formaldehyde Electrooxidation

Sungho Park,* Yong Xie, and Michael J. Weaver

Department of Chemistry, Purdue University, West Lafayette, Indiana 47907-1393

Received January 14, 2002. In Final Form: May 8, 2002

The voltammetric electrooxidation rates of formic acid, formaldehyde, and methanol in acidic electrolyte on carbon-supported platinum nanoparticle films with varying particle diameters (d) in the range of ca. 2−9 nm are examined with the objective of comparing the nanoparticle size sensitivity for these related yet distinct electrocatalytic processes. The reaction rates on the larger nanoparticles ($d > 4$ nm) are similar to those observed on polycrystalline Pt when normalized to the same microscopic Pt surface area. As noted previously, the rates of methanol electrooxidation decrease for Pt nanoparticle diameters below 4 nm. However, formic acid electrooxidation exhibits the opposite behavior, with rates *increasing* markedly for $d < 4$ nm, while formaldehyde electrooxidation displays little sensitivity to the Pt nanoparticle size. However, the extent of chemisorbed CO formation from all three reactants, as deduced from voltammetric and infrared spectral data, diminishes with decreasing d, the CO coverages for a given nanoparticle size being in the order methanol < formic acid < formaldehyde. These nanoparticle-size-dependent electrocatalytic and CO adsorptive findings are consistent with the occurrence of a Pt site "ensemble effect", where reactant dehydrogenation to form CO, and also in the case of formaldehyde and especially methanol to yield the reactive intermediate en route to CO_2 production, is impeded by the sharply decreasing availability of contiguous Pt terrace sites for $d < 4$ nm. This structural model is consistent with infrared measurements using CO as a nanoparticle structural probe, which show a rapidly decreasing proportion of terrace relative to edge Pt sites for $d < 4$ nm, in harmony with atomic packing considerations. The markedly enhanced electrocatalyic rates for formic acid oxidation on the smaller nanoparticles are attributed to the lack of a "Pt site ensemble" requirement for this process, coupled with decreased CO poisoning: unlike the other two reactions, oxygen addition (from coadsorbed −OH) is not necessarily required in order to produce CO_2 from formic acid.

Introduction

Understanding how the adsorptive and catalytic properties of metal nanoparticles depend on their size, structure, and local environment forms an intriguing theme in contemporary surface chemistry. While studies are less numerous so far, these issues are clearly of great interest in electrochemical systems, that is, for metal nanoparticle films acting as electrodes. Examples of the latter having substantial technological importance as well as fundamental significance are carbon-supported transition-metal nanoparticles, especially platinum, given their utilization in fuel-cell and other electrocatalytic-based devices.[1] Substantial efforts have been devoted to characterizing such C-supported Pt nanoparticles, especially in the diameter range of ca. 2−10 nm, including the utilization of X-ray absorption,[1,2] nuclear magnetic resonance (NMR),[3,4] and infrared spectroscopies.[4−7] This nanoparticle size range is of particular interest not only in view of its use in commercial applications but also because of the discernible changes in particle electronic and structural properties that are observed in this regime.[1−5] Thus, decreasing the Pt particle diameter, especially below ca. 5 nm, yields increases in the binding energy of CO, OH, and other adsorbates,[1,2] enhancements in the Fermi level density of states (DOS),[3,4] and red-shifts in the intramolecular stretching frequencies (ν_{CO}) for atop-bound CO adlayers.[4,5] The last property has been diagnosed as arising from marked increases in the proportion of edge relative to terrace sites, consistent with metal packing-geometry considerations.[5]

Especially given the availability of such detailed structural information, it is clearly of interest to explore the corresponding nanoparticle-size-dependent electrocatalytic properties. While several studies along these lines have been reported, they are limited for the most part to methanol oxidation[8,9] or oxygen reduction.[1,8b,10] Consistently, the rates of both these processes are observed to diminish progressively for smaller Pt nanoparticles, again most discernibly for $d \leq 5$ nm. These findings for methanol electrooxidation have been attributed to the stronger

* Corresponding author. E-mail: park37@purdue.edu.

(1) For example: McBreen, J.; Mukerjee, S. In *Interfacial Electrochemistry*; Wieckowski, A., Ed.; Marcel Dekker: New York, 1999; Chapter 49.

(2) (a) Mukerjee, S.; McBreen, J. *J. Electroanal. Chem.* **1998**, *448*, 163. (b) Bae, I. T.; Scherson, D. A. *J. Electrochem. Soc.* **1998**, *145*, 80.

(3) (a) Tong, Y. Y.; Rice, C.; Wieckowski, A.; Oldfield, E. *J. Am. Chem. Soc.* **2000**, *122*, 1123. (b) Tong, Y. Y.; Rice, C.; Wieckowski, A.; Oldfield, E. *J. Am. Chem. Soc.* **2000**, *122*, 11921.

(4) Rice, C.; Tong, Y. Y.; Oldfield, E.; Wieckowski, A.; Hahn, F.; Gloaguen, F.; Leger, J.-M.; Lamy, C. *J. Phys. Chem. B* **2000**, *104*, 5803.

(5) Park, S.; Wasileski, A.; Weaver, M. J. *J. Phys. Chem. B* **2001**, *105*, 9719.

(6) Park, S.; Tong, Y. Y.; Wieckowski, A.; Weaver, M. J. *Electrochem. Commun.* **2001**, *3*, 509.

(7) Park, S.; Tong, Y. Y.; Wieckowski, A.; Weaver, M. J. *Langmuir* **2002**, *18*, 3233.

(8) (a) Frelink, T.; Visscher, W.; van Veen, J. A. R. *J. Electroanal. Chem.* **1995**, *382*, 65. (b) Kabbabi, A.; Gloaguen, F.; Andolfatto, F.; Durand, R. *J. Electroanal. Chem.* **1994**, *373*, 251.

(9) For earlier related studies, see: (a) Yahikozawa, K.; Fujii, Y.; Matsuda, Y.; Nishimura, K.; Takasu, Y. *Electrochim. Acta* **1991**, *36*, 973. (b) Takasu, Y.; Fujii, Y.; Matsuda, Y. *Bull. Chem. Soc. Jpn.* **1986**, *59*, 3973.

(10) Kinoshita, K. *J. Electrochem. Soc.* **1990**, *137*, 845.

10.1021/la0200459 CCC: $22.00
Published on Web 06/19/2002

binding of OH and CO (formed by methanol surface decomposition) on smaller particles,[2a,8] and for oxygen reduction also by the greater stability of adsorbed OH found under these conditions.[2a]

To shed further light on these interesting nanoparticle-size-dependent electrocatalytic effects, it is desirable to compare the behavior of related reactions. An interesting trio of processes from this standpoint are the electrooxidation of methanol (CH_3OH), formaldehyde (HCOH), and formic acid (HCOOH), forming CO_2 in each case. The number of C−H bonds required to be cleaved diminishes in this sequence, and oxygen addition (probably from coadsorbed −OH) is necessarily required only for the first two processes.[11] Consequently, one would anticipate that the substrate structural requirements may be quite different for, say, methanol versus formic acid electrooxidation. This indeed turns out to be the case.[11]

Guided by this notion, we present here voltammetric data for the electrooxidation of methanol, formaldehyde, and formic acid on Pt nanoparticle films with diameters between ca. 2 and 9 nm, in comparison with the corresponding behavior on conventional polycrystalline platinum. Corresponding potential-dependent infrared data are also reported, primarily as a means of assaying the extent (and nature) of adsorbed CO formed from reactant surface dissociation (cf. ref 7). As described elsewhere,[5,6] we utilize thin C/Pt films formed (in the absence of Nafion or other fillers) by physical deposition onto gold substrates. Aside from displaying well-defined voltammetric characteristics, these ultrathin (1−2 Pt monolayer) films also yield near-ideal infrared reflection−absorption spectral (IRAS) properties. Interestingly, the findings indicate marked differences in the nanoparticle-size-dependent electrooxidation kinetics for the three reactions. These can be interpreted, at least qualitatively, on the basis of catalyst "ensemble effects", that is, in terms of differing requirements for multiple contiguous surface binding sites, depending on the surface oxidation pathway.[11,12]

Experimental Section

Most experimental details of the IRAS measurements are available elsewhere.[13] The FTIR spectrometer was a Mattson RS-2 instrument, with a custom-built external reflection compartment containing the narrow-band MCT detector. The spectral resolution was 4 cm^{-1}. The metal gold disk substrate (ca. 1.1 cm diameter), mounted on a glass plunger by wrapping with Teflon tape, was pressed against the CaF_2 window forming the base of the spectroelectrochemical cell so to create the optical thin layer.

The C/Pt films were prepared by depositing a dilute aqueous suspension (3 mg/mL) of the material (purchased from E-Tek, Inc, Natrick, MA) via a microsyringe onto the polished gold substrate.[5,6] The volume deposited, typically 10−50 μL, varied with the average film thickness desired. The suspension was then spread evenly over the surface by diluting with additional water droplets. While the gold surface was polished mechanically so to yield good infrared reflectivity, the provision of small "scratches" in the surface (formed, for example, by the pipet) aided the formation of a uniform aqueous film across the surface. The film was then dried by argon flow for ca. 3 min and rinsed with a jet of ultrapure water to remove loosely held particles. This last step is critical to obtaining good IRAS response; otherwise, some particles will "stick" to the thin-layer CaF_2 window, impairing the film integrity and stability. The resulting surface contains a thin, relatively uniform, and very reproducible C/Pt film which provides excellent voltammetric as well as IRAS characteristics, the latter being aided by its highly reflective nature.[5,6] Formic acid was 96% ACS Reagent Grade (Aldrich), and formaldehyde (26% aqueous solution, <1% methanol) was a gift from Monsanto-Pharmacia Corp. Carbon monoxide (99.99% min, Matheson Gases) was dispensed from an aluminum cylinder (to avoid iron carbonyl impurities), and supporting electrolytes were prepared from double-distilled H_2SO_4 (G.F. Smith) using ultrapure water from a Millipore MilliQ system. Electrode potentials are reported here versus the saturated calomel reference electrode, SCE (Bioanalytical Systems).

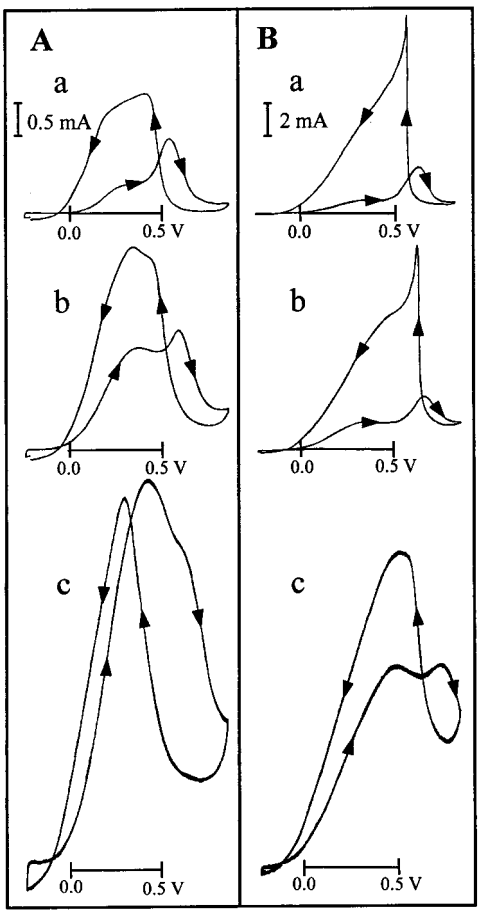

Figure 1. Cyclic voltammograms (50 mV s^{-1}) for electrooxidation of (A) 10 mM and (B) 0.1 M formic acid in 0.05 M H_2SO_4. Electrode surfaces: (a) polycrystalline Pt; (b) C/Pt (8.8 nm) nanoparticle film and (c) C/Pt (2.0 nm) film, both on Au substrates. The current scale given is normalized in each case to a 1 cm^2 Pt "effective area", corresponding to a H adsorption/desorption charge of 240 μC cm^{-2} (see text).

Results

The central purpose of this work is to examine, at least semiquantitatively, the electrooxidation rates of formic acid, formaldehyde, and methanol as a function of the Pt nanoparticle size. To this end, Figure 1 shows representative cyclic voltammograms obtained for the electrooxidation of 0.01 and 0.1 M formic acid (parts A and B, respectively) in 0.05 M H_2SO_4. The voltammograms labeled a in both cases refer to electrooxidation on a polycrystalline Pt surface. Voltammograms b and c were obtained on ultrathin C/Pt films with 60 and 10% Pt loading, respectively, corresponding to the average nanoparticle diameters of ca. 8.8 and 2.0 nm, as ascertained from transmission electron microscopy (TEM).[3] The current scales for each voltammogram, as indicated in curve

(11) For an erudite review, see: Jarvi, T. D.; Stuve, E. M. In *Electrocatalysis*; Lipkowski, J., Ross, P. N., Eds.; Wiley-VCH: New York, 1998; Chapter 3.

(12) For instructive discussions of the catalyst ensemble effect in heterogeneous catalysis, see: (a) Ross, P. N., Jr. In *Electrocatalysis*; Lipkowski, J., Ross, P. N., Eds.; Wiley-VCH: New York, 1998; Chapter 2. (b) Campbell, C. T. *Annu. Rev. Phys. Chem.* **1990**, *41*, 775.

(13) (a) Chang, S.-C.; Weaver, M. J. *J. Chem. Phys.* **1990**, *92*, 4582. (b) Tang, C.; Zou, S.; Severson, M. W.; Weaver, M. J. *J. Phys. Chem. B* **1998**, *102*, 8796.

a, refer to the unit (1 cm^2) area of the effective Pt surface area (on the polycrystalline Pt sample) as determined from characteristic hydrogen adsorption−desorption current−potential profiles below 0 V versus SCE.[5−7] (This hydrogen charge is 240 $\mu C\ cm^{-2}$.) The total surface area of the C/Pt films corresponds typically to 1−2 equivalent monolayers on this basis; this current normalization procedure facilitates comparison of their "intrinsic" electrocatalytic activities. Prior to adding the reactant, the Pt surfaces were cleaned by potential cycling for 1−2 min between −0.25 and 0.4 V, whereupon well-defined voltammetric features corresponding to adsorbed hydrogen and oxide formation/removal were obtained.[5,6] The voltammograms shown in Figure 1 each refer to an initial positive-going potential sweep (at 50 mV s^{-1}) starting from −0.2 V. However, similar voltammetric behavior was obtained for sweep rates between 10 and 100 mV s^{-1} and for initial potentials up to 0 V.

The voltammograms obtained on polycrystalline Pt (a) in Figure 1A,B contain familiar features, similar to those observed on monocrystalline surfaces such as Pt(110) where substantial CO coverages are formed.[14,15] Especially for the higher (0.1 M) reactant concentration (B) where CO production is more extensive (vide infra), only small anodic currents are observed during the initial positive-going potential sweep, at least at potentials, <0.4 to 0.5 V, prior to the oxidative removal of adsorbed CO. As usual, markedly larger anodic currents are observed during the return (negative-going) sweep, reflecting a relative lack of CO poisoning under these conditions.[11,14] Last, while the anodic currents are larger for the 10-fold higher formic acid concentration, the reaction orders are clearly well below unity, consistent with the occurrence of partial surface site blocking.

Inspection of the corresponding voltammetric data obtained on the nanoparticle Pt films, 8.8 and 2.0 nm in diameter, labeled b and c (again for 0.01 and 0.1 M formic acid concentrations in parts A and B of Figure 1, respectively), reveals interesting differences compared to the behavior on polycrystalline ("poly") Pt, curve a. Most strikingly, the electrooxidation currents increase markedly in the following order: poly ≤ 8.8 nm < 2.0 nm Pt particles. This trend is particularly marked during the initial positive-going sweep. Furthermore, the onset of formic acid oxidation on the smaller (2.0 nm) particles is sharper and occurs at a lower potential than on the larger particles, especially when compared to poly Pt (Figure 1). Intermediate voltammetric behavior was observed for C/Pt films with 2.5 and 3.2 nm diameter particles (i.e., 20 and 30% loading), with 4.0 nm particles (40% loading) yielding behavior close to that for the 8.8 nm samples (curve b in Figure 1). Therefore, essentially monotonic increases in electrocatalytic activity toward formic acid oxidation are seen as the Pt nanoparticle diameter is decreased.

Related, yet somewhat distinct, voltammetric behavior was observed for formaldehyde electrooxidation. Figure 2 contains such data obtained under the same conditions as in Figure 1, that is, for 0.01 and 0.1 M reactant concentrations (parts A and B), and on poly Pt and 8.8 and 2.0 nm Pt nanoparticles (curves a, b, and c, respectively). Similar to formic acid, formaldehyde electrooxidation exhibits higher currents during the reverse (negative-going) sweep, although significant oxidation during the positive-going sweep does not commence until higher potentials are reached, ca. 0.35−0.4 V (Figure 2). This

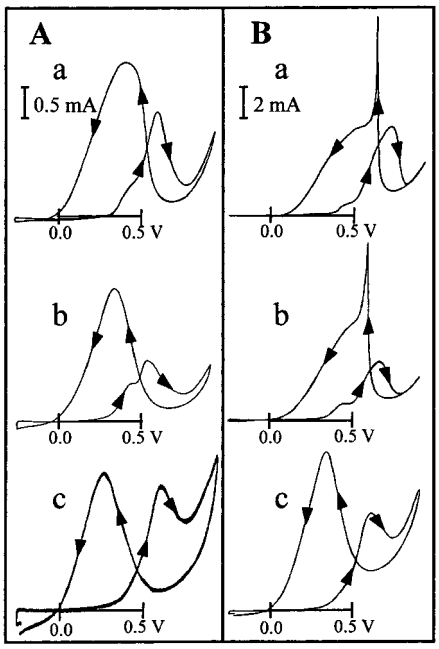

Figure 2. As in Figure 1, but for formaldehyde electrooxidation.

behavior is consistent with the substantial occurrence of catalytic site blocking by chemisorbed CO (vide infra). While the initial potential utilized in Figure 2 is again −0.2 V, essentially identical voltammograms were obtained for higher starting values, at least up to 0.2 V.

Unlike formic acid, however, the rates of formaldehyde electrooxidation are relatively insensitive to the Pt surface morphology, roughly similar responses being obtained for poly Pt and on the 8.8 and 2.0 nm Pt particles shown in Figure 2. This similarity extends to the intermediate-size Pt nanoparticle films just noted.

As in our earlier studies of small-molecule organic electrooxidation on monocrystalline (and polycrystalline) Pt-group surfaces,[14−20] acquiring real-time potential-dependent IRAS data during the voltammetric cycle can yield valuable information regarding the influence of chemisorbed CO on the electrooxidation process. The procedure that we have utilized previously entails acquiring a "reference spectrum" subsequently at a suitably high potential so that the CO is entirely removed (to form CO_2), thereby enabling absolute (i.e., unipolar) ν_{CO} spectra to be obtained over the electrocatalytically significant range of lower potentials (e.g., refs 14 and 21). A serious limitation of this procedure for the present C/Pt films, however, is that the substantial amounts of CO_2 produced (in the spectral thin layer) at higher potentials on the time scales (20−30 s) required for IRAS data acquisition tend to undermine the film integrity. A modified spectral referencing procedure was therefore utilized in the present work. This involves acquiring the reference spectrum *prior* to adding the reactant and waiting a sufficient time (ca. 15 min) for the species to diffuse from the surrounding solution reservoir into the spectral thin layer before acquiring "sample" spectra at the desired sequence of potentials.

(14) For example: Chang, S.-C.; Leung, L.-W.; Weaver, M. J. *J. Phys. Chem.* **1990**, *94*, 6013.
(15) Chang, S.-C.; Ho, Y.; Weaver, M. J. *Surf. Sci.* **1992**, *265*, 81.
(16) Chang, S.-C.; Hamelin, A.; Weaver, M. J. *J. Chim. Phys.* **1991**, *88*, 1615.
(17) Leung, L.-W. H.; Weaver, M. J. *J. Phys. Chem.* **1989**, *93*, 7218.
(18) Kizhakevariam, N.; Weaver, M. J. *Surf. Sci.* **1994**, *310*, 183.
(19) Gomez, R.; Weaver, M. J. *J. Electroanal. Chem.* **1997**, *435*, 205.
(20) (a) Corrigan, D. S.; Weaver, M. J. *J. Electroanal. Chem.* **1988**, *241*, 143. (b) Leung, L.-W. H.; Weaver, M. J. *Langmuir* **1990**, *6*, 323.
(21) Corrigan, D. S.; Leung, L.-W. H.; Weaver, M. J. *Anal. Chem.* **1988**, *239*, 55.

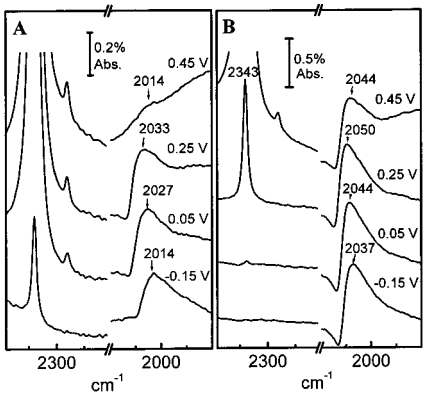

Figure 3. Selected potential-dependent IRAS absorbance spectra acquired on a C/Pt (8.8 nm) film in (A) 10 mM formic acid and (B) 10 mM formaldehyde, both with 0.05 M H_2SO_4. The reference spectrum in both cases was obtained (using 100 interferometer scans) at the initial potential (−0.15 V vs SCE) prior to adding the reactant. The corresponding sample spectra were obtained after waiting for a sufficient period (15 min) for the reactant to diffuse into the thin-layer cavity and then stepping the potential in 0.1 V positive increments, holding for ca. 30 s at each value.

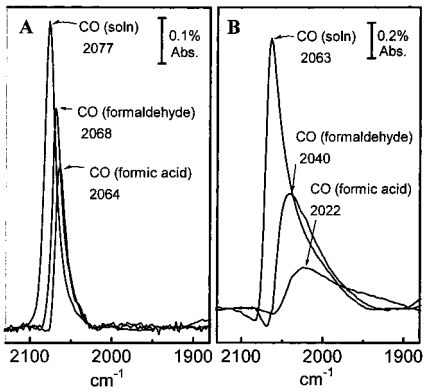

Figure 4. Representative IRAS absorbance spetcra obtained at −0.05 V vs SCE on (A) polycrystalline Pt and (B) C/Pt (8.8 nm) film for chemisorbed CO formed from saturated solution CO, 10 mM formaldehyde, and 10 mM formic acid, as indicated, each in 0.05 M H_2SO_4. Spectra were acquired similarly to those in Figure 3.

Figure 3A,B shows representative potential-dependent IRAS absorbance spectra obtained in this fashion on C/Pt (8.8 nm) films for 10 mM formic acid (A) and formaldehyde (B), again in 0.05 M H_2SO_4 electrolyte. The data were acquired during a "staircase" potential excursion with 0.1 V increments, pausing a sufficient time (ca. 30 s) at each potential to record a set of 100 interferometer scans. As expected, two major spectral features appear in the wavenumber region (1800−2500 cm^{-1}) shown. The broad band peaked at 2015−2050 cm^{-1} seen in both parts A and B of Figure 3 is readily assigned to the C−O stretching (ν_{CO}) of atop-chemisorbed CO. While this feature is broader and red-shifted from the band frequencies observed for atop CO on conventional Pt electrodes, as discussed in ref 5 (and below), its appearance is consistent with adsorption on the C/Pt nanoparticles. (Note that the small negative-going band component seen especially in part B is due not to residual CO in the reference spectrum but rather to the "anomalous" optical properties of the C/Pt films.[6]) The spectra produced from formaldehyde display more intense ν_{CO} bands having higher peak frequencies, consistent with the formation of higher CO coverages than is the case from formic acid. In addition, the ν_{CO} band is retained to significantly higher potentials in the presence of formaldehyde (ca. 0.5 V) as compared to formic acid (ca. 0.35 V). The other feature seen in Figure 3A,B, an intense band appearing at 2345 cm^{-1}, signals the formation of CO_2 , trapped in the thin layer on this time scale.[21] In harmony with the voltammograms shown in Figure 1A (curve b) and Figure 2A (curve b), the onset of CO_2 production from the organic electrooxidation is seen from the infrared data to occur at higher potentials with formaldehyde than formic acid.

Further information as to the nature and extent of chemisorbed CO formed under these conditions can be gleaned by comparing the ν_{CO} bands on a common absorbance scale with corresponding IRAS data for adlayers produced from solution CO itself. Figure 4 compares ν_{CO} spectra obtained at −0.05 V for a saturated adlayer (i.e., for unit coverage, $\theta_{CO} = 1$) formed upon exposure to saturated solution CO with those formed in the presence of 10 mM formic acid and formaldehyde, as indicated, under the same conditions. The left-hand segment (A) refers to polycrystalline Pt, whereas the right-hand portion (B) was obtained for a C/Pt (8.8 nm) film. The broader and red-shifted nature of the ν_{CO} bands obtained on the C/Pt films compared with the poly Pt substrate is clearly evident in Figure 4. Given that the integrated ν_{CO} absorbances should be roughly proportional to the CO coverage,[13b] the θ_{CO} values for formaldehyde and especially formic acid under these conditions are deduced to be below saturation, particularly on the C/Pt nanoparticle films (Figure 4B). Corresponding IRAS spectra to Figures 3 and 4 were also obtained for C/Pt films with 2.5 and 2 nm nanoparticles. These spectra (not shown) exhibit weaker ν_{CO} bands with lower peak frequencies. Normalization with corresponding spectral intensities for adlayers formed by solution CO dosing[4] (defined here as $\theta_{CO} = 1$) indicates that lower θ_{CO} values are formed from formic acid and formaldehyde than on the largest (8.8 nm) nanoparticle films. The issue of CO coverages is considered further below.

As noted at the outset, the comparison of the electrooxidation rates for methanol with the reactants just described is of central interest here. Figure 5 shows representative voltammetric data for methanol oxidation, obtained under the same conditions as for formic acid (Figure 1) and formaldehyde (Figure 2). Thus, segments A and B refer to 0.01 and 0.1 M methanol concentrations, and the voltammograms labeled a, b, and c were obtained on poly Pt and on C/Pt films with 8.8 and 2.0 nm nanoparticles, respectively. Inspection of Figure 5 shows that the dependences of the methanol electrooxidation rates on the Pt surface morphology are quite different from those observed for formaldehyde and especially formic acid. In particular, the methanol oxidation rate *decrease* in the sequence poly > 8.8 nm > 2.0 nm Pt (Figure 5) is in contrast to the marked current *increases* seen in the same order for formic acid electrooxidation (Figure 1). Again, voltammograms obtained on the intermediate-size nanoparticle films followed the same trend, so that the methanol oxidation rates diminished monotonically with decreasing nanoparticle diameter, at least for $d \leq 4$ nm, consistent with the earlier reports noted above.[8] Comparable voltammograms were obtained for methanol dosing at potentials in the range from −0.2 to 0.1 V, as observed for formaldehyde electrooxidation (vide supra). Perhaps surprisingly, the voltammetric currents do not increase greatly (only ca. 2-fold or less) when changing the methanol concentration from 0.01 to 0.1 M (Figure 5A,B), indicating an apparent limitation in the availability of catalytic surface sites.

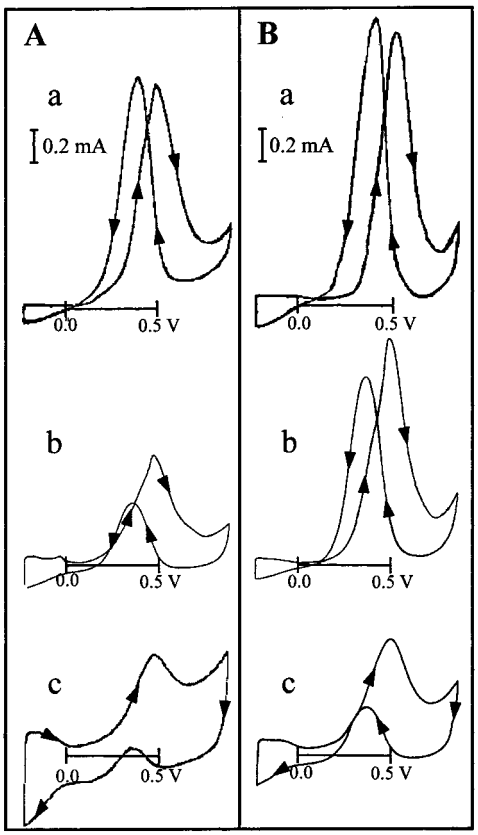

Figure 5. As in Figure 1, but for methanol electrooxidation.

Potential-dependent IRAS measurements were also undertaken with methanol in the same fashion as described above. However, we encountered difficulties in obtaining "absolute" ν_{CO} spectra when using the procedure utilized to obtain Figures 3 and 4; that is, by acquiring a reference spectrum before introducing methanol into the spectral thin layer via diffusion. Nevertheless, (bipolar) ν_{CO} difference spectra could be obtained for a pair of potentials in the region, −0.2 to 0.2 V, below the onset of methanol electrooxidation. These results are reported in detail in ref 7. They indicate that only intermediate CO coverages are formed by methanol dosing, the θ_{CO} values being lower on the smallest nanoparticles.

As a further means of assaying the extent of chemisorbed CO formation under reaction conditions for each system, we undertook voltammetric experiments following removal of the reactant by repeated flushing with supporting electrolyte while holding the potential at a fixed value. The dashed traces in Figure 6A,B show representative voltammograms obtained (at 50 mV s^{-1}) in this fashion after exposure to 10 mM formic acid and formaldehyde in 0.05 M H_2SO_4 at −0.2 V and subsequent solution flushing. The reactant exposure time, ca. 3 min, was chosen so to roughly match the conditions used in Figures 1 and 2. Segments a and b refer to C/Pt films with 8.8 and 2.5 nm nanoparticles, respectively. (The current scale shown refers to the values obtained on the gold substrates employed, having a geometric area of 0.95 cm^2.) The solid traces show the corresponding voltammograms obtained in the absence of adsorbed CO.

Approximate estimates of the fractional CO coverage, θ_{CO} (where saturation is taken as $\theta_{CO} = 1$), can be obtained from these data in two ways. The first method entails measuring the extent to which the hydrogen adsorption−desorption charge (in the −0.2 to 0.1 V region) is attenuated relative to the complete removal obtained following dosing

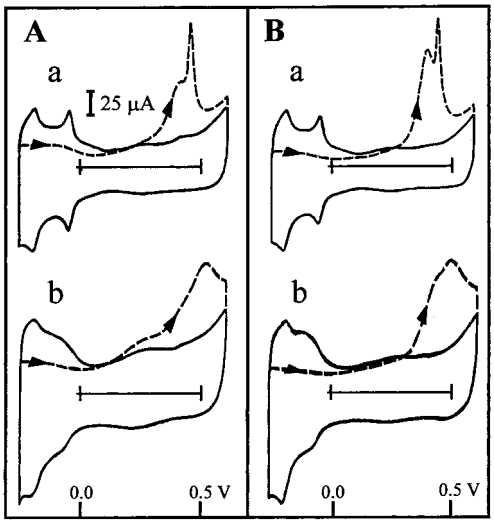

Figure 6. Anodic voltammograms (50 mV s^{-1}) for removal of adsorbed species (chiefly CO) following exposure of C/Pt films with (a) 8.8 nm and (b) 2.5 nm Pt nanoparticles to (A) 10 mM formic acid and (B) 10 mM formaldehyde, both in 0.05 H_2SO_4 at −0.2 V vs SCE, and subsequent solution flushing with supporting electrolyte (dashed traces). The solid traces are corresponding cyclic voltammograms obtained following adsorbate removal. The geometric area of the gold substrate was 0.95 cm^2.

Table 1. Nanoparticle−CO Packing Densities Formed by Reactant Dosing[a]

particle diameter (nm)	θco (methanol)	θco (formic acid)	θco (formaldehyde)
8.8	0.3	0.6	0.8
2.5	<0.2	0.5	0.6
2.0	<0.2	0.3	0.4

[a] The CO coverage relation to saturation, θ_{co}, refers to exposure of the C/Pt films, as indicated, to 10 mM reactant in 0.05 M H_2SO_4 for 2−3 min at −0.2 V. The solution was then replaced with supporting electrolyte by repeated flushing. The θ_{co} values were determined from the voltammetric charge for CO electrooxidation (Figure 6) normalized to the value for a saturated adlayer formed similarly by solution CO dosing.

with solution CO (cf. ref 7). The second method involves measuring the anodic charge for irreversible CO electrooxidation, as obtained from the anodic wave located at 0.3−0.6 V (Figure 6) with respect to the corresponding charge for a saturated CO layer, again produced by solution CO dosing (cf. ref 5). Both of these tactics yielded similar θ_{CO} estimates (within ca. 20%) for formic acid and formaldehyde dosing, although the latter method gave significantly lower θ_{CO} values upon methanol exposure. This latter finding, which suggests the presence of additional chemisorbed species beyond chemisorbed CO and H, is similar to that found for methanol adsorption on low-index Pt electrodes.[14]

Resulting θ_{CO} estimates based on the CO electrooxidation charge are summarized in Table 1 for three Pt nanoparticle diameters, 8.8, 2.5, and 2.0 nm. Significantly, (20−50%) higher θ_{CO} values are obtained by increasing the reactant dosing time, say to 30−60 min, for larger reactant concentrations and at higher dosing potentials. The effect of increasing the dosing potential on the resulting θ_{CO} values is most marked with methanol. (Qualitatively similar results have been recently reported elsewhere.[22]) However, the θ_{CO} values in Table 1 are considered to be most relevant to the cyclic voltammetric

(22) Jusys, Z.; Behm, R. J. *J. Phys. Chem. B* **2001**, *105*, 10874.

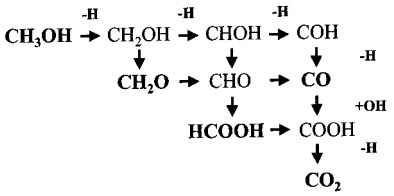

Figure 7. Schematic ladder-matrix mechanism, showing possible adsorbed intermediates, extracted from ref 25 (see also ref 11).

data presented in Figures 1, 2, and 5. (Note that suppressing the CO coverage is also desirable from a kinetic interpretative standpoint.) While the θ_{CO} values are necessarily only approximate, two trends evident in Table 1 are of significance here. First, the extent of chemisorbed CO formation for a given C/Pt film decreases in the order formaldehyde > formic acid > methanol. Second, for all three reactants the extent of CO production diminishes with decreasing nanoparticle size. These trends are consistent with the IRAS data presented above and in ref 7.

Discussion

When examined in conjunction with the corresponding extent of chemisorbed CO formation (Table 1), along with the Pt nanoparticle structure as gleaned from related IRAS data,[5] the distinct nanoparticle-size-induced changes in voltammetric oxidation rates of formic acid and methanol provide evidence for the occurrence of differing types of reaction pathways. The likely reaction mechanisms for formic acid and methanol electrooxidation on Pt-group metals, especially platinum itself, have been discussed at considerable length, bolstered by the availability of detailed kinetic and spectroscopic data on ordered single-crystal electrodes.[11,12a,23] Although chemisorbed CO formed by reactant dissociation can provide a significant route to CO_2 under some conditions,[24] the commonly accepted mechanism for these processes considers CO to constitute a relatively nonreactive or even "poisoning" moiety, the reaction occurring instead via the parallel formation of more weakly chemisorbing species.[11] Since the direct spectral detection and especially the clear identification of the latter species have been problematic, deductions of likely reaction pathways have relied primarily on kinetic-based evidence.[11,12a,23]

Two related aspects of the mechanistic insight so deduced are of particular relevance here. First, a likely difference between the electrooxidation pathway for formic acid as compared with formaldehyde and methanol, already mentioned, is that the addition of oxygen (most likely from OH coadsorbed in an adjacent site) to form the CO_2 product is clearly required for the latter two processes but not necessarily for the first. This difference is clearly evident from the "ladder-scheme" mechanism of stepwise dehydrogenation−oxygenation, due originally to Bagotzky et al.,[25] summarized for these three reactants in Figure 7. Note that in addition to the stepwise ladder matrix shown, other adsorbed intermediates may be envisaged. In particular, adsorbed formate (HCOO) rather than the carboxylic acid fragment shown (COOH) (i.e., involving initial C−H rather than O−H cleavage) may constitute the major reaction intermediate to formic acid electrooxidation.[11,26] Indeed, direct IRAS evidence supporting this contention has been obtained on low-index iridium electrodes.[19]

Second, an interesting consequence of the *sequential* C-dehydrogenation steps needed to oxidize formaldehyde and especially methanol is that the presence of multiple contiguous surface sites should be required for only the first two processes and not necessarily for formic acid. The need for such multiple binding sites has been explored in detail, originally for catalysis at metal−gaseous systems[12b] and later also for an electrocatalytic process,[11,12a] by modifying Pt-group surfaces with varying coverages of metal adatoms. While such additives may also influence reaction rates via electronic and other factors, there is strong evidence that the primary effect of some adatoms (e.g., Bi, Pb) is indeed to markedly diminish the availability of contiguous surface sites, commonly known as the ensemble effect.[12]

An example of the ensemble effect that is particularly germane to the present systems involves the influence of Bi adatoms on formic acid and methanol electrooxidation at Pt(111) and Pt(100), examined earlier in our laboratory by combined electrochemical−IRAS measurements.[15] The presence of increasing Bi coverages, θ_{Bi}, on Pt(100) was found to yield sharp decreases in the CO coverage formed by formic acid dissociation (θ_{CO} approaching zero for $\theta_{Bi} > 0.2$), together with marked increases in the electrooxidation rates. The former observation can readily be accounted for in terms of an ensemble effect, given that the dehydration of formic acid to yield CO should require at least two adjacent (ensemble) binding sites, the availability of which will decline sharply with increasing θ_{Bi}.[15] The concomitant enhancements in the rates of formic acid electrooxidation to CO_2 seen with increasing θ_{Bi} can be accounted for (at least partially) from the *increases* in available catalytic sites freed up by the decreases in θ_{CO}, provided that generation or reaction of the *reactive* intermediate does not require the same Pt atom ensemble. A deduction that the formic acid electrooxidation rates are even enhanced upon decreasing the Pt ensemble size was reached from kinetic measurements on stepped Pt(111) surfaces also modified by Bi adatoms.[27]

Interestingly, the rates of methanol electrooxidation on Pt(100) *decrease* for increasing θ_{Bi}, even though the (admittedly smaller) θ_{CO} values are also attenuated under these conditions, again so that $\theta_{CO} \rightarrow 0$ for $\theta_{Bi} > 0.2$.[15] Although not originally interpreted as such,[15] this behavior strongly suggests that the reactive intermediate for CO_2 production and the chemisorbed CO formed by methanol dissociation require an ensemble of catalytic sites, so that both pathways are impaired severely upon the addition of Bi adatoms.

The central point of this paper is to suggest that a similar ensemble effect is also operative with the present Pt nanoparticles, specifically that the availability of contiguous Pt terrace sites is diminished progressively as the particle diameter d is decreased. Key evidence favoring this nanoparticle structural interpretation is obtained from our d-dependent IRAS data for CO chemisorption via solution CO dosing.[5] These results show that the fraction of Pt "flat terrace" versus edge sites on the nanoparticle surface declines sharply for $d \leq 4$ nm, as gleaned primarily from the progressive ν_{CO} red-shifts seen for atop CO under these conditions.[5] Such structural alterations, along with systematic changes in the ν_{CO}−

(23) (a) Hamnett, A. In *Interfacial Electrochemistry*; Wieckowski, A., Ed.; Marcel Dekker: New York, 1999; Chapter 47. (b) Parsons, R.; VanderNoot, T. *J. Electroanal. Chem.* **1988**, *257*, 9.
(24) Mrozek, M. F.; Luo, H.; Weaver, M. J. *Langmuir* **2000**, *16*, 8463.
(25) Bagotzky, V. S.; Vassiliev, Yu, B.; Khazora, O. A. *J. Electroanal. Chem.* **1977**, *81*, 229.
(26) Lamy, C.; Leger, J. M. *J. Chem. Phys.* **1991**, *88*, 1649.
(27) Smith, S. P. E.; Abruna, H. D. *J. Electroanal. Chem.* **1999**, *467*, 43.

electrode potential dependences observed for intermediate θ_{CO} values, signal the progressive diminution in the presence of 9-coordinate terrace sites along with the emerging dominance of lower-coordinate Pt surface atoms, as d decreases from ca. 4 to 2 nm. Interestingly, these nanoparticle structural changes are consistent with the size-dependent configurations anticipated for icosahedra and related close-packed arrangements.[28] Examination of the icosahedral geometries (as detailed in ref 28) shows that the probability of finding two or more adjacent terrace Pt atoms is sharply diminished on smaller nanoparticles in this size range. For example, the 8.8 nm particle offers ca. 5-fold greater availability of adjacent Pt atoms in a $\sqrt{3}$ geometry (probably suitable for reacting coadsorbates) than is the case for the 2.5 nm particle.

At least on a qualitative basis, then, such size-dependent changes in the nanoparticle surface structure can readily account for the essential features of the present electrocatalytic and adsorptive behavior. The progressively smaller extent of chemisorbed CO production from dissociation of all three reactants with diminishing nanoparticle diameter (Table 1) can be attributed to the decreasing availability of contiguous terrace binding sites, given that C−H bond cleavage should be facilitated by the availability of an adjacent Pt site to bind the H atom. Although the dissociation of methanol to CO, for example, is facilitated to some extent at step sites, such as on Pt(533) [i.e., 4(111) × (100),[29] the nanoparticle edge sites mark points of sharp surface "curvature", where the availability of two-dimensional Pt site ensembles is terminated. The relative ineffectiveness of such sites for reactant dissociation is therefore not surprising.

Furthermore, the qualitatively different dependence of the rates of formic acid and methanol electrooxidation on the nanoparticle size (Figures 1 and 5) can readily be rationalized on this basis. The smaller electrocatalytic activity for the latter process on the smallest nanoparticles (d < 4 nm) is consistent with the anticipated diminished capability of generating the reactive intermediate, probably −COH or −CHO,[11] by methanol dissociation (Figure 7), given the similar anticipated need for Pt site ensembles as for chemisorbed CO formation. If the production of CO_2 from formic acid electrooxidation, as argued above, does not require Pt site ensembles, the smaller extent of CO poisoning seen on the smallest nanoparticles should facilitate the reaction, in harmony with the markedly *greater* electrocatalytic activity seen for d < 4 nm (Figure 1). The relative insensitivity of the formaldehyde electrooxidation rates to the nanoparticle size (Figure 1) can be rationalized on the basis of offsetting effects. On one hand, the diminution in θ_{CO} seen for decreasing nanoparticle diameter (Table 1) should facilitate the reaction given that the extent of CO poison formation expected from the θ_{CO} values should then be moderated. (Note that the inhibiting influence of the chemisorbed CO is clearly evident in Figure 2 from the onset of significant electrooxidation during the initial positive-going sweep only at potentials, <0.4 V, where CO is oxidized.) On the other hand, the production of the reactive intermediate (probably −CHO) from formaldehyde dehydrogenation will also be inhibited due to the decreasing availability of site ensembles on the smallest nanoparticles, thereby yielding an offsetting effect on the overall electrocatalysis. Last, the comparable electrocatalytic properties of the 8.8 nm nanoparticles in comparison with polycrystalline Pt for all three reactions examined here (Figures 1, 2, and 5) are also consistent with these structural considerations, given the prevalence of flat terraces on the larger particles, as deduced from the IRAS properties of chemisorbed CO.[5]

The present interpretation of nanoparticle-size effects on methanol electrocatalysis differs from that of earlier studies, where the diminished activity on the smaller Pt nanoparticles was attributed to the apparently stronger adsorption of OH and CO observed under these conditions,[2a,8] resulting in a decreased availability of Pt surface sites and/or a lower oxidizing ability of the −OH species. However, the latter notions do not provide an explanation of the differing nanoparticle size dependence seen here for formic acid (or formaldehyde) electrooxidation. Nevertheless, the possibility that an ensemble effect is also responsible was mentioned in ref 8b.

Concluding Remarks

Admittedly, the present interpretation of the observed sensitivity of electrocatalytic activity on Pt nanoparticle films to the particle size in terms of a "catalyst ensemble effect" is only qualitative in nature, limited in part by the present incomplete information on their detailed microscopic structure. However, a key virtue of this study lies in the *comparative* examination of catalytic nanoparticle size effects for related, yet structurally distinct, C_1 organic reactants. More specifically, the markedly differing behavior of formic acid versus methanol electrooxidation under these conditions, coupled with corresponding trends in the extent of chemisorbed CO formation, enables mechanistic/structural deductions to be made that would clearly not be feasible by examining only a single reaction. The likely mechanistic differences between these two processes have been stressed earlier; indeed, the conclusion has been reached that the formic acid reaction does not serve as a useful "model" of the key aspects of methanol electrocatalysis.[11] While this point of view is unassailably correct in a sense, the consequence of the differing features of the electrooxidation pathways in their sensitivity to experimental variables, in the present case the nanoparticle size, can also be extremely instructive from a mechanistic standpoint.

Given the present results, it would appear worthwhile to pursue more quantitative studies of nanoparticle-size/structure effects in electrocatalysis (for example, on a single-crystalline surface, see ref 30). While the present C/Pt materials are of direct technological importance, limitations include their significant polydisperse nature (i.e., nonuniform particle sizes) along with the possibility of carbon-support effects on their electronic properties.[3] For these reasons, it would clearly be desirable to explore such metal nanoparticle structural effects for more "ideal", preferably monodisperse, films. In addition, the adsorptive and electrocatalytic examination of bimetallic and other modified nanoparticles formed by controlled deposition tactics, analogous to those well established for conventional electrode surfaces, should be very instructive. Studies along these lines are being pursued in our laboratory.

Acknowledgment. This work is supported by the National Science Foundation (Analytical and Surface Chemistry Program) and by Monsanto-Pharmacia Corp. via the Purdue Chemistry Industrial Associates Program.

LA0200459

(28) Benfield, R. E. *J. Chem. Soc., Faraday Trans.* **1992**, *88*, 1107.
(29) Shin, J.; Korzeniewski, C. *J. Phys. Chem.* **1995**, *99*, 3419.
(30) Sriramulu, S.; Jarvi, T. D.; Stuve, E. M. *J. Electroanal. Chem.* **1999**, *467*, 132.